Radioprotection 2019, 54(2), 117–123

https://doi.org/10.1051/radiopro/2019011

Available online at:
www.radioprotection.org

ARTICLE

Evaluation of CT calibration curves from stoichiometric and tissue substitute methods according to tissue characteristics

I. Amini[1,2,3] and P. Akhlaghi[1,2,*]

[1] Immunology Research Center, Tabriz University of Medical Sciences, Tabriz, Iran.
[2] Department of Medical Physics, School of Medicine, Tabriz University of Medical Sciences, Tabriz, Iran.
[3] Students' Research Committee, Tabriz University of Medical Sciences, Tabriz, Iran.

Received: 3 June 2018 / Accepted: 10 April 2019

Abstract – In order to optimize and increase the precision of dose determination, it is important to obtain the relationship between CT Hounsfield units and electron densities, as the basic inputs for radiotherapy planning systems. Therefore, the aim of this study was to plot and compare the CT calibration curves resulted from both tissue substitute calibration (based on the tissue equivalent materials) and stoichiometric calibration (based on biological tissues) methods for a specific CT scanner at tube voltage of 120 kVp by applying a precise homemade physical phantom. Hence, the Hounsfield units of all phantom materials were measured experimentally and also calculated by related formulas. Considering the CT numbers and the electron densities of various tissue equivalent materials and real tissues, the calibration curves were plotted. According to the results, the higher accuracy of the stoichiometric method relative to tissue substitute method was confirmed in this study. On the other hand, since estimating Hounsfield unit of each human tissue strongly depends on the physical properties of tissue substitutes of the physical phantom, the high precision of this phantom led to increase the accuracy of the calibration curves obtained based on the stoichiometric method.

Keywords: CT calibration curve / electron density / physical phantom / stoichiometric calibration / tissue substitute method

1 Introduction

Calculation of dose within the targeted volume is an essential step in radiotherapy treatment planning systems (Schneider *et al.*, 2000). Many factors such as inhomogeneity and overlapping of patient's body tissues have effects on the dose distribution (Skrzyński *et al.*, 2010). Frequently, X-ray computed tomography (CT) is used in radiotherapy treatment planning systems as a basic source of information about the exact anatomical locations of the inhomogeneities to correct tissue heterogeneities (Cozzi *et al.*, 1998). Since CT scans are worked at diagnostic X-ray energies (up to 140 kVp), the CT numbers or Hounsfield units (HUs) should be converted into physical properties of human tissues (such as electron densities), before they become applicable for calculating doses at higher X-ray energies (Yang *et al.*, 2008). The correlation between the CT numbers, and electron densities (ρ_e) of different tissues (CT calibration curve), is the prerequisite for accurate patient dose calculations in radiotherapy treatment planning systems (Yang *et al.*, 2008; Tsukihara *et al.*, 2015). The common method of displaying this calibration curve is tissue substitute method, in which, a number of different tissue equivalent materials with known physical properties is selected and scanned by desired CT scanner. As a result, the CT number values of these materials are extracted and according to their electron densities, the calibration curve is plotted (Constantinou *et al.*, 1992). After this report, the errors in the determining the relationship of HUs to electron densities caused by differences in the physical and chemical properties of tissue equivalent materials with those of real tissues were illustrated. Hence, to improve the calibration method, stoichiometric calibration was presented and its higher accuracy was demonstrated by Schneider *et al.* (1996). In this method, at first, using the appropriate tissue equivalent materials and mathematical equations, a general relationship for a specific CT scanner is obtained to predict the CT number of each substance with the specified characteristics. Then, applying the obtained relationship, the CT numbers of real tissues are calculated and according to their electron densities values, the calibration curve is plotted. So far, many researchers have used these two methods to find the

*Corresponding author: parissa_akhlaghi@yahoo.com

relationship between CT number and electron density (Yang *et al.*, 2008; Yohannes *et al.*, 2011); but for the first time the tissue substitute method and stoichiometric method were presented and used by Constantinou *et al.* (1992) and Schneider *et al.* (1996), respectively.

Two factors are very effective on increasing the accuracy of the stoichiometric calibration:

1. The accuracy and precision of the tissue equivalent materials that are initially used to obtain a general relationship. Therefore, the different international phantoms are designed and constructed (*e.g.* http://www.cirsinc.com/products/all/24/electron-density-phantom, and http://www.rsdphantoms.com). In this regard, Amini *et al.* (2018) was designed and fabricated a physical phantom of adult chest region that could be used for dosimetry and calibration purposes (Amini *et al.*, 2018).

2. Whereas, the measured CT numbers might vary in different CT scanners, separate calibration curves should be considered for various CT scanners. The type of scanner can strongly influence the calibration, so that, 10% deviation is observed in electron density depending on the type of scanner (Constantinou *et al.*, 1992). Once the calibration curves at different scan protocols of a particular CT scanner are obtained, they could be used in all centers that intend to benefit from these scanner data.

Considering the importance of calibration curves in treatment planning systems, the purpose of this paper is investigating both stoichiometric and tissue substitute methods for a specific CT scanner (Siemens SOMATOM sensation 64-slice scanner) at common tube voltage of chest scan (120 kVp) using of a homemade physical chest phantom (Amini *et al.*, 2018). The calibration curves for other tube voltages (80, 100, and 140 kVp) were also obtained.

2 Materials and Methods

2.1 CT scan parameters

All measurements were performed on a Siemens SOMATOM sensation 64-slice CT scanner (Iran Radiology Center, Tabriz, Iran). Based on this scanner protocols reported on https://www.ctisus.com/, in most chest scan the tube voltage of 120 kVp is selected for different applications. Therefore, slice thickness of 1 mm, tube voltage of 120 kVp and tube loading of 220 mAs were considered. Moreover, the field of view diameter and pixel size were 382 and 0.746 mm, respectively.

2.2 Physical phantom

An elliptical calibration physical phantom was designed and built based on a cross-sectional slice of adult human chest. The phantom body was made of Polymethylmethacrylate (PMMA) with thickness of 5 cm, small diameter of 27 cm, and large diameter of 33 cm. Seventeen holes with 3 cm diameter were considered for embedding different tissue equivalent materials. According to the physical properties (mass density, electron density and effective atomic number) of real tissues in chest region, water, Polyurethane foam, Polypropylene, Polyethylene, Acrylonitrile butadiene styrene, Polyurethane, Polyamide and Polyoxymethylene were selected and prepared for replacement of water, lungs (in both inhale and exhale modes), adipose, breasts, muscle, liver, cartilage and ribs, respectively (Fig. 1) (Amini *et al.*, 2018).

2.3 Measurement of CT number

The averaged CT numbers were acquired for a manually defined region of interest (ROI) with an area of 3 cm^2 using E-film software (https://estore.merge.com/na/index.aspx), which helps users to display, analyze and process CT images. Each ROI was considered in the middle of each material away from the edges to avoid partial volume effects influencing the results (Inness *et al.*, 2014). Given that two locations were assigned for each material, the average HUs of these two sites was considered as final HU of that material (Amini *et al.*, 2018).

2.4 Calculation of CT number

As known, CT images provide information about the radiation attenuation coefficients in form of CT numbers, expressed in HUs, as follow:

$$\mathrm{HU} = \left(\frac{\mu}{\mu_{\mathrm{H_2O}}} - 1\right) \times 1000, \tag{1}$$

where μ is linear attenuation coefficient and $\mu_{\mathrm{H_2O}}$ is the linear attenuation coefficient of water. The total linear attenuation coefficient of photon in diagnostic energy range is calculated by the summation of photonic cross sections multiplied by the electron density (Jackson and Hawkes, 1981). As shown, for a mixture of elements, photonic cross sections depend on K_{KN}, K_{ph} and K_{sca} constant coefficients, which are related to Klein-Nishina cross-section, photon absorption and photon scattering cross-section, respectively (Rutherford *et al.*, 1976; Schneider *et al.*, 1996; Yohannes *et al.*, 2012), so;

$$\overline{\mu} = \rho N_A \sum\nolimits_{i=1}^{n} \left(\frac{w_i}{A_i}\overline{\mathrm{K}}^{\mathrm{KN}}\left(Z_i + Z_i^{2.86}\frac{\overline{\mathrm{K}}^{\mathrm{sca}}}{\overline{\mathrm{K}}^{\mathrm{KN}}} + Z_i^{4.62}\frac{\overline{\mathrm{K}}^{\mathrm{ph}}}{\overline{\mathrm{K}}^{\mathrm{KN}}}\right)\right), \tag{2}$$

where N_A, W_i, Z_i and A_i are Avogadro's number, elemental weight fraction, atomic number and atomic mass of each element, respectively. To simplify, we considered the ratio of $\frac{\overline{\mathrm{K}}^{\mathrm{sca}}}{\overline{\mathrm{K}}^{\mathrm{KN}}}$ as constant k_1 and the ratio of $\frac{\overline{\mathrm{K}}^{\mathrm{ph}}}{\overline{\mathrm{K}}^{\mathrm{KN}}}$ as constant k_2.

Considering equation (1), to obtain HU of any arbitrary material, the relative attenuation coefficient of that material $\left(\frac{\overline{\mu}}{\overline{\mu}_{\mathrm{H_2O}}}\right)$ should be defined. Therefore, using equation (2) and elemental composition of water (H_2O), the relative attenuation coefficient of each material was obtained as below:

$$\frac{\overline{\mu}}{\overline{\mu}_{\mathrm{H_2O}}} = \frac{\rho}{\rho_{\mathrm{H_2O}}} \frac{\sum_{i=1}^{n}(w_i/A_i)\left(Z_i + Z_i^{2.86}\,\mathrm{k}_1 + Z_i^{4.62}\,\mathrm{k}_2\right)}{(w_H/A_H)\left(1 + \mathrm{k}_1 + \mathrm{k}_2\right) + (w_O/A_O)\left(8 + 8^{2.86}\,\mathrm{k}_1 + 8^{4.62}\,\mathrm{k}_2\right)}. \tag{3}$$

Real tissue	Equivalent material	Chemical composition and weight fraction in percent of tissue equivalent material				Location
		H_1	C_6	N_7	O_8	
Water	Water	11.19	-	-	88.81	1
Lung (exhale)	Polyurethane foam (exhale)	6.94	67.27	8.31	17.00	2
Lung (inhale)	Polyurethane foam (inhale)	6.94	67.27	8.31	17.00	3
Breast	Polyethylene	14.37	85.63	-	-	4
Ribs	Polyoxymethylene	6.71	40.00	-	53.28	5
Cartilage	Polyamide	9.80	63.69	12.38	14.14	6
Liver	Polyurethane	9.07	64.35	6.00	20.57	7
Muscle	Acrylonitrile butadiene styrene	8.11	85.26	6.63	-	8
Adipose	Polypropylene	14.37	85.63	-	-	9
Body	Polymethylmethacrylate	8.05	59.98	-	31.96	10

Fig. 1. Physical chest phantom together with the chemical composition of each tissue equivalent material for use in calibration and dosimetry applications (Amini *et al.*, 2018).

In the equation (3), if k_1 and k_2 are known, $\frac{\overline{\mu}}{\overline{\mu}_{H_2O}}$ and therefore CT number of each material with specified chemical composition could be calculated (Schneider *et al.*, 2000). So, given equation (1), using measured value of HU and also the composition and density of each material, the constants of k_1 and k_2 were determined empirically by a linear regression fit. As a result of chi-square goodness of fit test, the obtained k_1 and k_2 values minimized the relation $\sum_{n=1}^{10}\left[\left(\frac{\overline{\mu}}{\overline{\mu}_{H_2O}}(k_1 \cdot k_2)\right)_n - \left(\frac{HU(meas.)}{1000}+1\right)_n\right]^2$. Therefore, the HU of each phantom material calculated by these two constants, had the smallest difference with the measured value. According to that fact that, k_1 and k_2 values depend on the CT machine, so, once they were determined by this statistical method, HU of any arbitrary tissue (like real human tissue) with specified chemical composition could also be obtained. Finally, by considering these k_1 and k_2 values in equation (3) and using equation (1), a general relationship was obtained for Siemens SOMATOM Sensation 64-slice CT scanner at tube voltage of 120 kVp in order to calculate the CT number of each substance with a specific chemical composition. The general relationships for other tube voltages were also obtained using the mentioned method.

2.5 Electron density

Relative electron density (number of electrons per gram) of each material was calculated according to its mass density and chemical composition, as below:

$$\rho_e = \frac{\rho N_g}{\rho_{water} N_{g_{water}}}, \quad (4)$$

where ρ is mass density (in gram per unit volume) and N_g is the number of electrons per unit volume of material and was determined by (Schneider *et al.*, 1996):

$$N_g = N_A \sum_{n=1}^{i} \frac{w_i Z_i}{A_i}, \quad (5)$$

where N_A is Avogadro's number, W_i, Z_i and A_i are elemental weight fraction, atomic number and atomic mass of each element, respectively. The electron densities of tissue equivalent materials were provided in Table 1.

2.6 Tissue substitute calibration

To plot the calibration curve based on tissue substitutes method and investigate the effects of choosing different materials on final calibration curve, various tissue equivalent materials with known physical properties and densities in the range of those of real human tissues were selected (ICRU, 1989). For these materials, the CT number and electron density were calculated from equations (1) and (4), respectively. Then, the calibration curve was plotted at tube voltage of 120 kVp.

2.7 Stoichiometric calibration

In this method, given the obtained general relationship for calculating the CT number of each substance with a specific chemical composition, the CT numbers of different human real tissues were also determined (Schneider *et al.*, 1996). In addition, the electron densities of these materials were calculated using equation (4). Finally, the calibration curve for real tissues was plotted.

2.8 Phantom accuracy

To investigate the accuracy of using this homemade physical phantom in plotting the calibration curves, 11 real bone tissues of Table 2 (cortical bone, cranium, femur, humerus, mandible, ribs (2nd, 6th), ribs (10th), sacrum, spongiosa, vertebral column (c4), vertebral column (D6, L3)) and six bone substitutes of Table 1 (B-110, Milenex, Magnesium, Polytetrafluoroethylene, Polyvinyl chloride, SB5) were selected. Then, for the current study and also three other studies (Schneider *et al.*, 1996; Vanderstraeten *et al.*, 2007; Shih and Wu, 2017), the following steps were taken:

- by placing the constants of k_1 and k_2 in equation (3) and using equation (1), the CT numbers of those 11 real bone materials and 6 bone substitutes were calculated. Then, according to their electron densities, the calibration curves were plotted;
- a linear fit was resulted from calibration with an equation in the form of $y = ax + b$, in which x is CT number and y is electron density;

Table 1. Mass density, electron density and the calculated CT numbers of tissue equivalent materials (for tissue substitute method) at tube voltage of 120 kVp of Siemens SOMATOM sensation 64-slice scanner.

Tissue equivalent material	ρ(g/cm^3)	ρ_e(e$^-$/g)	CT number
A-150	1.12	1.11	96.09
Acrylic	1.17	1.14	119.76
Alderson–lung	0.32	0.30	−692.86
Alderson–muscle A	1.00	0.98	−25.90
Alderson–muscle B	1.00	0.98	−18.95
AP6	0.91	0.88	−129.63
AP/L2	0.92	0.93	−80.58
AP/SF1	0.92	0.93	−92.98
B-100	1.45	1.38	534.54
B-110	1.79	1.65	956.25
BR12	0.97	0.95	−78.18
Ethoxyethanol	0.93	0.93	−84.87
EVA-28	0.95	0.96	−63.93
Frigerio gel	1.12	1.11	106.00
Frigerio liquid	1.08	1.07	71.44
Glycerol trioleate	0.92	0.92	−97.07
Goodman liquid	1.07	1.06	57.23
Griffith breast	1.10	1.08	69.25
Griffith lung	0.26	0.25	−747.19
Griffith muscle	1.12	1.10	91.62
M3	1.05	1.05	46.26
Magnesium	1.74	1.55	751.25
Melinex	1.40	1.31	297.40
Polyamide	1.13	1.11	93.72
Paraffin wax	0.93	0.96	−66.24
Plaster of Paris	2.32	2.13	1641.20
Polyethylene	0.92	0.95	−80.75
Polystyrene	1.05	1.02	−7.76
Polytetrafluoroethylene	2.10	1.82	855.18
Polyvinyl chloride	1.35	1.24	516.41
RF-1	0.93	0.95	−68.63
Rice powder	0.84	0.81	−203.89
RM-1	1.03	1.04	34.42
RM/G1	1.07	1.06	60.79
RM/L3	1.04	1.03	30.33
RM/SR4	1.03	1.02	0.19
Rossi gel	1.10	1.09	82.22
Rossi liquid	1.11	1.10	92.09
RW-1	0.90	0.99	−20.27
SB5	1.87	1.77	1152.27
White liquid	1.72	1.60	913.45
WT1	1.02	0.99	−10.11

Table 2. Mass density, electron density and the calculated CT numbers of real human tissues (for stoichiometric method) at tube voltage of 120 kVp of Siemens SOMATOM sensation 64-slice scanner.

Real tissue	ρ(g/cm^3)	ρ_e(e$^-$/g)	CT number
Adipose tissue	0.95	0.95	−65.06
Blood	1.06	1.05	52.19
Brain	1.04	1.03	35.27
Breast	1.02	1.01	5.79
Cell nucleus	1.00	0.99	−1.16
Eye lens	1.07	1.05	51.02
Gastrointestinal tract	1.03	1.02	23.07
Heart	1.06	1.05	52.69
Kidney	1.05	1.04	41.59
Liver	1.06	1.05	59.67
Lung (deflated)	1.05	1.04	42.41
Lung (inflated)	0.26	0.26	−741.87
Lymph	1.03	1.03	27.16
Muscle	1.05	1.04	40.68
Ovary	1.05	1.04	43.88
Pancreas	1.04	1.03	32.08
Cartilage	1.10	1.08	92.03
Red marrow	1.03	1.02	15.00
Yellow marrow	0.98	0.98	−36.13
Skin	1.09	1.08	75.00
Spleen	1.06	1.05	52.12
Testis	1.04	1.03	34.42
Thyroid	1.05	1.04	66.26
Cortical bone	1.92	1.78	1196.47
Cranium	1.61	1.52	773.60
Femur	1.33	1.28	429.94
Humerus	1.46	1.39	602.55
Mandible	1.68	1.58	868.09
Ribs (2nd, 6th)	1.41	1.35	515.24
Ribs (10th)	1.52	1.44	671.32
Sacrum	1.29	1.24	357.14
Spongiosa	1.18	1.15	229.14
Vertebral (C4)	1.42	1.35	550.14
Vertebral (D6, L3)	1.33	1.28	417.90

– four CT numbers in the bone region were selected, optionally (400, 600, 800 and 1000), and for each CT number, the electron density was predicted using the linear equations.

3 Results

3.1 k_1 and k_2 values

As a result of goodness of fitness test with least squares method, the constants of k_1 and k_2, at 120 kVp tube voltage were obtained 1.08×10^{-3} and 1.07×10^{-5}, respectively for Siemens Somatom Sensation 64-slice scanner.

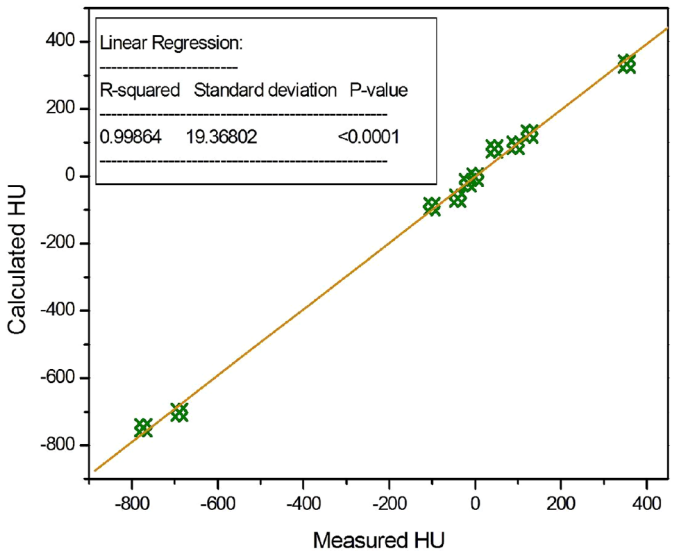

Fig. 2. The graph of calculated *versus* measured CT numbers of phantom materials at tube voltage of 120 kVp.

3.2 Measured and calculated CT numbers of phantom materials

The graph of calculated CT numbers relative to measured CT numbers of phantom materials was plotted in Figure 2. The result of goodness of linear fit along the 45-degree diagonal line (R-squared values are higher than 0.998) with standard deviation of 19.36 and maximum deviation of 36.97 indicates the good agreements.

3.3 CT calibration curves

The outcomes of calculating the CT numbers of tissue equivalent materials (for tissue substitute method) and real tissues (for stoichiometric method) together with their electron densities were provided in Tables 1 and 2, respectively. Figure 3 displays the calibration curves for both groups of tissue equivalent materials (tissue substitute method) and real tissues (stoichiometric method) at 120 kVp tube voltage.

In this figure, the solid line (A) is the calibration curve resulted from the stoichiometric method. Also, the dotted and dashed lines (B and C) are calibration curves plotted based on tissue substitute method. In curve B, the materials of Melinex, Polytetrafluoroethylene, PMMA, and in curve C, magnesium, SB5, Plaster of Paris were considered as bone substitutes, in addition lung and soft tissue substitutes introduced by ICRU were used for both curves. Given curve A, the data points representing real tissues (stars) fall on a smooth curve and data dispersion is low (stoichiometric method), so there is a single calibration curve based on stoichiometric method. While, the curves plotted based on tissue substitute method strongly depend on the types of tissue equivalent materials. As a result, for lung and soft tissues (mass density less than 1.2 g/cm^3), the data dispersion is low and there is a single calibration curve, but by increasing mass density and approaching to bone densities, the dispersion of data points (squares) increases.

In Table 3 the linear equations obtained for real bone tissues and bone substitutes to predict the electron density

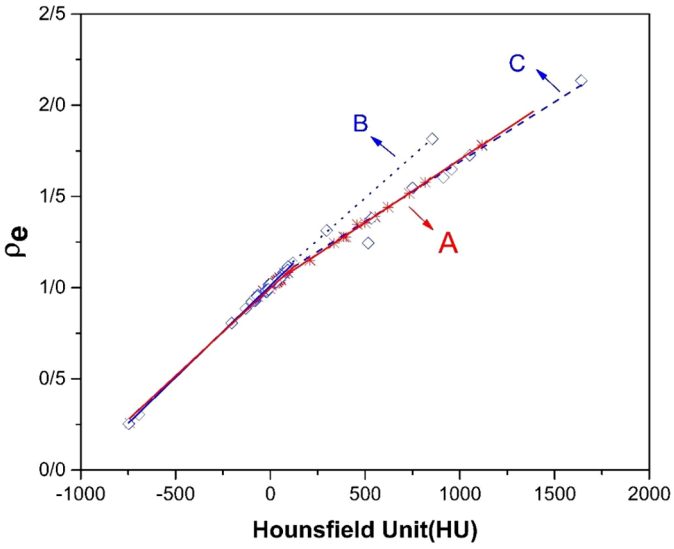

Fig. 3. Calibration curves for Siemens SOMATOM Sensation 64-slice CT scanner at tube voltage of 120 kVp. The solid line (A) with star data points results from the stoichiometric method and the dotted and dashed lines (B and C) with squares eventuate from the tissue substitute method.

Table 3. The linear fit equations for real bone tissues group (RB) and bone substitutes group (SB) in this study and three other studies at tube voltage of 120 kVp.

Study	Linear fit equation
Schneider *et al.* (1996)	$y_{RB} = 5.65 \times 10^{-4}\, x + 1.01$
	$y_{SB} = 4.42 \times 10^{-4}\, x + 1.16$
Vanderstraeten *et al.* (2007)	$y_{RB} = 5.93 \times 10^{-4}\, x + 1.00$
	$y_{SB} = 4.73 \times 10^{-4}\, x + 1.15$
Shih and Wu (2017)	$y_{RB} = 5.58 \times 10^{-4}\, x + 1.00$
	$y_{SB} = 4.09 \times 10^{-4}\, x + 1.19$
Current study	$y_{RB} = 6.54 \times 10^{-4}\, x + 1.00$
	$y_{SB} = 6.27 \times 10^{-4}\, x + 1.07$

values were tabulated. Moreover, the relative difference between the electron densities obtained from two linear equations of each study was determined in Table 4. Given the comparisons, the obtained relative differences were 3.77, 6.20, 4.96 and 5.04, in this study and the studies of Shih and Wu (2017), Vanderstraeten *et al.* (2007) and Schneider *et al.* (1996), respectively.

4 Discussion

In this study, the CT calibration curves for two groups of real tissues introduced by Schneider *et al.* (1996),(stoichiometric method) and tissue equivalent materials provided by ICRU (tissue substitute method) were investigated. In this regard, based on the chemical composition of each material/tissue, the electron densities and also the CT numbers for

Table 4. The relative difference in the electron density from two methods obtained in this study and three other studies.

Selected CT number	Study			
	Schneider *et al.* (1996)	Vanderstraeten *et al.* (2007)	Shih and Wu (2017)	Current study
400	8.06	8.31	10.54	4.90
600	6.09	5.89	7.41	4.08
800	3.91	3.72	4.83	3.34
1000	2.10	1.94	2.02	2.77

mentioned groups were determined. In Figure 3, the use of different tissue equivalent materials as the bone substitutes leads to different calibration curves in tissue substitute method (curves B and C), as expected. It could be said that the stoichiometric calibration performed based on the hand-made physical phantom of this study, is more precise than tissue substitute method in plotting the calibration curve.

Given the high price of physical phantom available in the market, designing and constructing a precise physical phantom with tissue equivalent materials close to real human tissues selected from available polymers, such as the physical chest phantom applied in this study, helps users to provide calibration curves for different scanners and protocols.

Given Table 4, it is observed that the relative difference between two calibration methods in this study is less than three other studies, which confirms high compliance of tissue equivalent materials of the applied physical phantom to the real human tissues in terms of physical properties. Moreover, the results of this investigation have the most similarity to those of Vanderstraeten *et al.* (2007), which is due to the fact that same CT scanner and similar physical phantom was used in both studies. While, due to the differences between phantoms and also scanners, discrepancies with two other studies are higher.

Treatment planning systems that intend to use Siemens Somatom Sensation 64-slice scanner data could consider the resulted calibration curve of this investigation. The calibration curves determined based on real human tissues are clearly more accurate than calibration curves obtained from various groups of tissue equivalent materials. Stoichiometric method makes it possible to provide a single curve as an input for different treatment planning systems.

It should be mentioned that the constants of k_1 and k_2, which directly determine the CT number of each material, relate to the physical properties and chemical compositions of tissue substitutes of the scanned physical phantom. Hence, applying this kind of precise physical phantom and the process described in this investigation, this study could be easily expanded to other scan protocols and CT scanners, so a library of these calibration curves at common protocols may assist and improve dosimetric aspects of radiotherapy treatment planning systems.

5 Conclusion

The aim of this study was to investigate two common calibration methods using a homemade precise physical

phantom for dose optimization in radiotherapy treatment planning systems. The results indicated that in low mass densities (lung and soft tissues), there was no significant difference between the curves obtained from two methods, but by increasing the densities and approaching to bone densities, the differences were revealed. As observed, considering different materials as bone substitutes led to the different results in calibration curve of tissue substitute method. While, in stoichiometric method and for real tissues, there was one single calibration curve. Therefore, it is suggested to use precise physical phantom and stoichiometric method in order to plot the calibration curves for various treatment planning systems. On the other hand, the comparisons between the outcomes of this project and three other studies confirmed the higher similarity between the tissue equivalent materials and the real human tissues in this study. This phantom provided more accurate general relationships for predicting CT numbers of different materials, and thus more accurate calibration curve based on the stoichiometric method.

Acknowledgments. This research is financially supported by a grant from the Immunology Research Center, Tabriz University of Medical Sciences, Tabriz, Iran. The authors like to acknowledge Mr Yaghoob Khaleghifard the head radiologist of Iran Radiology Center in Tabriz for his cooperation in imaging the constructed phantom.

References

Amini I, Akhlaghi P, Sarbakhsh P. 2018. Construction and verification of a physical chest phantom from suitable tissue equivalent materials for computed tomography examinations. *Radiat. Phys. Chem.* 150: 51–57.

Constantinou C, Harrington JC, DeWerd LA. 1992. An electron density calibration phantom for CT-based treatment planning computers. *Med. Phys.* 19: 325–327.

Cozzi L, Fogliata A, Buffa F, Bieri S. 1998. Dosimetric impact of computed tomography calibration on a commercial treatment planning system for external radiation therapy. *Radiother. Oncol.* 48: 335–338.

Inness EK, Moutrie V, Charles PH. 2014. The dependence of computed tomography number to relative electron density conversion on phantom geometry and its impact on planned dose. *Australas. Phys. Eng. Sci. Med.* 37: 385–391.

International Commission on Radiation Units and Measurement. 1989. Tissue substitutes in radiation dosimetry and measurement. *ICRU Rep. 44* 41: 1–220.

Jackson DF, Hawkes DJ. 1981. X-ray attenuation coefficients of elements and mixtures. *Phys. Rep.* 70: 169–233.

Rutherford R, Pullan B, Isherwood I. 1976. Measurement of effective atomic number and electron density using an EMI scanner. *Neuroradiology* 11: 15–21.

Schneider U, Pedroni E, Lomax A. 1996. The calibration of CT Hounsfield units for radiotherapy treatment planning. *Phys. Med. Biol.* 41: 111–124.

Schneider W, Bortfeld T, Schlegel W. 2000. Correlation between CT numbers and tissue parameters needed for Monte Carlo simulations of clinical dose distributions. *Phys. Med. Biol.* 45: 459–478.

Shih CT, Wu J. 2017. Converting computed tomography images into photon interaction coefficients by using stoichiometric calibration and parametric fit models. *Med. Phys.* 44: 510–521.

Skrzyński W, Zielińska-Dąbrowska S, Wachowicz M, S lusarczyk-Kacprzyk W, Kukołowicz PF, Bulski W. 2010. Computed tomography as a source of electron density information for radiation treatment planning. *Strahlenther. Onkol.* 186: 327–333.

Tsukihara M, Noto Y, Sasamoto R, Hayakawa T, Saito M. 2015. Initial implementation of the conversion from the energy-subtracted CT number to electron density in tissue inhomogeneity corrections: An anthropomorphic phantom study of radiotherapy treatment planning. *Med. Phys.* 42: 1378–1388.

Vanderstraeten B *et al*. 2007. Conversion of CT numbers into tissue parameters for Monte Carlo dose calculations: A multi-centre study. *Phys. Med. Biol.* 52: 539–562.

Yang M, Virshup G, Mohan R, Shaw CC, Zhu XR, Dong L. 2008. Improving accuracy of electron density measurement in the presence of metallic implants using orthovoltage computed tomography. *Med. Phys.* 35: 1932–1941.

Yohannes I, Kolditz D, Kalender WA. 2011. Semiempirical analysis of materials' elemental composition to formulate tissue-equivalent materials: A preliminary study. *Phys. Med. Biol.* 56: 2963–2977.

Yohannes I, Kolditz D, Langner O, Kalender WA. 2012. A formulation of tissue-and water-equivalent materials using the stoichiometric analysis method for CT-number calibration in radiotherapy treatment planning. *Phys. Med. Biol.* 57: 1173–1190.

Cite this article as: Amini I, Akhlaghi P. 2019. Evaluation of CT calibration curves from stoichiometric and tissue substitute methods according to tissue characteristics. *Radioprotection* 54(2): 117–123